Compressibility and crystal structure of kyanite, Al_2SiO_5, at high pressure

HEXIONG YANG, ROBERT T. DOWNS, LARRY W. FINGER, ROBERT M. HAZEN, AND
CHARLES T. PREWITT

Geophysical Laboratory, 5251 Broad Branch Road, NW, Washington, DC 20015-1305, U.S.A.

ABSTRACT

The unit-cell dimensions and crystal structure of kyanite at various pressures up to 4.56 GPa were refined from single-crystal X-ray diffraction data. The bulk modulus is 193(1) GPa, assuming $K' = 4.0$. Calculated unit-strain tensors show that kyanite exhibits more isotropic compressibility than andalusite or sillimanite. The most and least compressible directions in the kyanite structure correspond approximately to the most and the least thermally expandable directions. The analysis of the distortion of the closest packing in kyanite indicates that the most compressible direction of the structure (along [012]) corresponds to the direction along which the closest-packed O monolayers are stacked. The bulk moduli for the Al1, Al2, Al3, and Al4 octahedra are 274(43), 207(14), 224(26), and 281(24) GPa, respectively, and those for the Si1 and Si2 tetrahedra are 322(80) and 400(95) GPa, respectively. Four AlO_6 octahedra that all become less distorted at higher pressures do not display clearly dominant compression directions. The average unshared O-O distance for each octahedron is considerably more compressible than the shared O-O distance. The high-pressure behaviors of the Al1 and Al4 octahedra are very similar but different from those of the Al2 and Al3 octahedra. Bulk moduli for the three Al_2SiO_5 polymorphs (kyanite, sillimanite, and andalusite), as well as those for the AlO_6 octahedra in their structures, appear to decrease linearly as their volumes increase. The significantly larger bulk modulus and more isotropic compressibility for kyanite than for andalusite or sillimanite are a consequence of the nearly cubic close-packed arrangement of O atoms and the complex edge-sharing among four distinct AlO_6 octahedra in the kyanite structure.

INTRODUCTION

The three Al_2SiO_5 polymorphs (kyanite, sillimanite, and andalusite) are of paramount importance in metamorphic and experimental petrology because of their abundance in metamorphosed pelitic rocks and relatively simple chemistry. Furthermore, they provide an interesting crystal-chemical system. On the one hand, all these structures have Si exclusively in tetrahedral coordination and one-half of the total Al in octahedral coordination. These AlO_6 octahedra share edges to form chains running parallel to the *c* axis. On the other hand, the remaining Al is fourfold, fivefold, and sixfold coordinated in sillimanite, andalusite, and kyanite, respectively. A knowledge of the crystal structures of these polymorphs as a function of pressure is therefore essential in understanding the stability relationships and phase-transition mechanisms within the Al_2SiO_5 system.

Relative to sillimanite and andalusite, kyanite is the high-pressure phase in the Al_2SiO_5 system. The crystal structure of kyanite was first deduced by Náray-Szabo et al. (1929) from the structure determination of staurolite and refined by Burnham (1963) from single-crystal X-ray diffraction data. It can be considered as a distorted cubic close-packed arrangement of O atoms, with 10% of the tetrahedral sites filled with Si and 40% of the octahedral sites filled with Al. The fact that kyanite is 12–14% denser than sillimanite and andalusite is partly attributable to this close-packing feature. There are four crystallographically distinct Al sites (Al1, Al2, Al3, and Al4) and two Si sites (Si1 and Si2) (Fig. 1). The Al1 and Al2 sites are in the zigzag edge-sharing octahedral chains. The chains are cross-linked by alternating SiO_4 tetrahedra and AlO_6 octahedra with Si1 and Al4 on one side and Si2 and Al3 on the other. The Al1 and Al3 octahedra share five edges with neighboring octahedra, whereas Al2 and Al4 share four edges with adjacent octahedra. Winter and Ghose (1979) studied the structural variations of kyanite, sillimanite, and andalusite with temperature. Ralph et al. (1984) determined the compressibility and the crystal structure of andalusite at pressures up to 3.7 GPa. Studies on the crystal structures of the three Al_2SiO_5 polymorphs have been summarized by Papike and Cameron (1976), Winter and Ghose (1979), Ribbe (1980), and Kerrick (1990). In this paper, we compare our high-pressure structure study of kyanite (up to 4.56 GPa) with other studies of andalusite at high pressures to better understand the crystal chemistry of the Al_2SiO_5 system at high pressure.
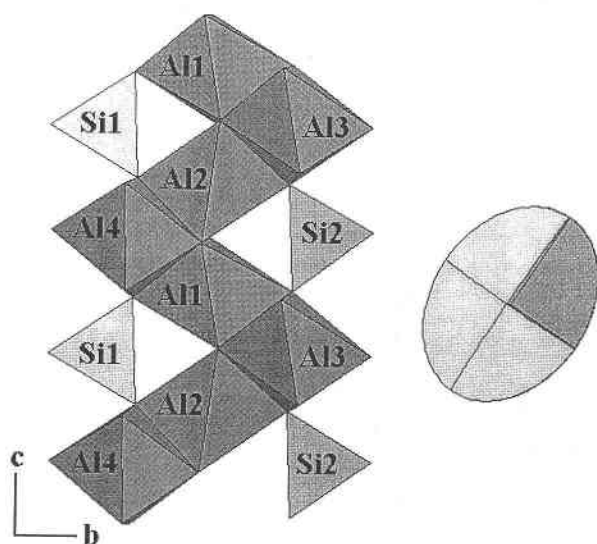
FIGURE 1. Crystal structure of kyanite. Note zigzag chains of edge-shared AlO_6 octahedra running parallel to c. The strain ellipsoid was calculated using the unit-cell parameters at 4.56 GPa relative to those at room pressure.

EXPERIMENTAL PROCEDURES

Room-pressure X-ray diffraction measurements

The sample used in this study is from Minas Gerais, Brazil and was kindly supplied by Pete J. Dunn of the Smithsonian Institution (specimen no. NMNH 139740). It was used by Skinner et al. (1961) for determination of unit-cell dimensions, and by Robie and Hemingway (1984) and Hemingway et al. (1991) for low-temperature heat-capacity measurements. Several samples were crushed and carefully searched for fragments suitable for a high-pressure single-crystal X-ray diffraction study. However, as noticed by Winter and Ghose (1979), severely bent crystals were very common, probably resulting from the crushing. Finally, a single-crystal fragment (0.10 × 0.09 × 0.04 mm) was selected that showed sharp diffraction profiles and minimum diffuse background. A Picker four-circle diffractometer equipped with a Mo X-ray tube (β-filtered) was used for all X-ray measurements. Unit-cell parameters were determined by fitting the positions of 20 reflections in the range $20° < 2θ <$ 35° following the procedure of King and Finger (1979), yielding $a = 7.1200(4)$, $b = 7.8479(3)$, $c = 5.5738(3)$ Å, $α = 89.974(3)$, $β = 101.117(4)$, and $γ = 106.000(4)°$ (Table 1). These values are close to those reported by Skinner et al. (1961) for the same material from powder X-ray diffraction: $a = 7.124(2)$, $b = 7.850(2)$, $c = 5.567(2)$ Å, $α = 89.92(1)$, $β = 101.27(1)$, and $γ = 106.00(1)°$.

X-ray intensity data from a hemisphere of reciprocal space with $0° ≤ 2θ ≤ 60°$ were collected using ω scans of 1° width in step increments of 0.025° and 3 s per step counting time. Two standard reflections were checked every 5 h; no significant or systematic variations in intensities of the standard reflections were observed. Digitized step data were integrated by the method of Lehmann and Larsen (1974) using an option to reset backgrounds manually when necessary. Corrections were made for Lorentz and polarization effects but not for X-ray absorption by the crystal ($μ = 12.38$ cm^{-1}). The total number of measured reflections was 1835, out of which there were 1545 reflections with $I > 3σ_I$, where $σ_I$ is the standard deviation determined from the counting statistics.

The initial structural model of kyanite was taken from Winter and Ghose (1979). Least-squares refinements were performed in the space group $P\bar{1}$ using an updated version of RFINE4 (Finger and Prince 1975). Neutral atomic scattering factors, including anomalous dispersion corrections for Al, Si, and O, were taken from *International Tables for X-ray Crystallography*, Ibers and Hamilton (1974). Weighting schemes were based on $w = 1/[σ_F^2 + (pF)^2]$, where p is adjusted to ensure that the errors were normally distributed through probability plot analysis (Ibers and Hamilton 1974). Type II isotropic extinction corrections (Becker and Coppens 1975) were applied in the refinements. Atomic positional coordinates and displacement parameters are presented in Table 2.

High-pressure X-ray diffraction measurements

After the collection of X-ray intensity data at room pressure, the crystal was mounted in a Merrill-Bassett diamond-anvil cell with a mixture of 4:1 methanol:ethanol as the pressure medium. Four small (~10 μm) ruby chips were included as the internal pressure calibrant (Mao et al. 1986) from which pressure was determined

TABLE 1. Crystal data and other relevant information on kyanite at various pressures

P (GPa)	a (Å)	b (Å)	c (Å)	α (°)	β (°)	γ (°)	V (Å³)	Total refls.	Refls. >3σ_I	R_int	R_w	R
0.00*	7.1200(4)	7.8479(3)	5.5738(3)	89.974(3)	101.117(4)	106.000(4)	293.31(2)	1835	1545		0.019	0.016
0.68	7.1132(6)	7.8401(6)	5.5672(6)	89.995(7)	101.111(8)	106.002(6)	292.42(5)					
1.35*	7.1038(7)	7.8305(5)	5.5605(6)	90.023(8)	101.112(9)	106.001(6)	291.28(5)	1037	340	0.035	0.028	0.029
1.98	7.0960(7)	7.8229(6)	5.5544(6)	90.027(8)	101.098(9)	105.994(7)	290.38(5)					
2.54*	7.0896(4)	7.8173(4)	5.5497(4)	90.031(5)	101.098(5)	105.987(5)	289.68(3)	1032	343	0.033	0.025	0.026
3.10	7.0823(5)	7.8096(5)	5.5432(6)	90.057(6)	101.091(7)	105.987(6)	288.79(4)					
3.73*	7.0750(6)	7.8027(6)	5.5367(6)	90.063(7)	101.091(8)	105.985(6)	287.87(5)	1024	334	0.035	0.033	0.032
4.32	7.0677(6)	7.7955(4)	5.5325(5)	90.076(6)	101.088(7)	105.984(5)	287.09(4)					
4.56*	7.0648(5)	7.7926(4)	5.5299(6)	90.089(7)	101.085(7)	105.982(5)	286.73(4)	1021	331	0.034	0.031	0.029

* X-ray intensity data were collected at these pressures.

TABLE 2. Atomic positional and isotropic displacement parameters of kyanite at various pressures

Atom		0.00	1.35	2.54	3.73	4.56
				P (GPa)		
Al1	*x*	0.32533(5)	0.3249(5)	0.3245(5)	0.3241(6)	0.3243(6)
	y	0.70412(4)	0.7041(4)	0.7038(4)	0.7034(4)	0.7035(4)
	z	0.45812(6)	0.4581(8)	0.4572(7)	0.4560(8)	0.4565(8)
	B_{iso}	0.267(7)	0.43(3)	0.42(3)	0.41(4)	0.39(3)
Al2	*x*	0.29740(5)	0.2972(5)	0.2973(5)	0.2985(6)	0.2976(6)
	y	0.69882(4)	0.6989(4)	0.6990(4)	0.6994(4)	0.6988(4)
	z	0.95040(6)	0.9499(8)	0.9507(7)	0.9524(8)	0.9503(8)
	B_{iso}	0.258(7)	0.35(3)	0.38(3)	0.36(3)	0.38(3)
Al3	*x*	0.09980(5)	0.0996(5)	0.0997(5)	0.1001(6)	0.0998(6)
	y	0.38615(4)	0.3861(4)	0.3862(4)	0.3866(4)	0.3861(4)
	z	0.64043(6)	0.6405(8)	0.6408(7)	0.6413(7)	0.6403(8)
	B_{iso}	0.259(7)	0.37(3)	0.40(3)	0.34(3)	0.37(3)
Al4	*x*	0.11205(5)	0.1114(5)	0.1116(5)	0.1124(5)	0.1123(5)
	y	0.91750(4)	0.9171(4)	0.9170(3)	0.9176(4)	0.9178(4)
	z	0.16469(6)	0.1639(7)	0.1642(7)	0.1652(7)	0.1649(7)
	B_{iso}	0.273(7)	0.37(3)	0.42(3)	0.36(4)	0.33(4)
Si1	*x*	0.29625(5)	0.2964(5)	0.2964(4)	0.2959(5)	0.2963(5)
	y	0.06488(4)	0.0647(3)	0.0646(3)	0.0650(4)	0.0651(3)
	z	0.70657(5)	0.7067(8)	0.7057(6)	0.7054(7)	0.7056(7)
	B_{iso}	0.215(6)	0.38(3)	0.36(3)	0.33(3)	0.34(3)
Si2	*x*	0.29102(5)	0.2922(4)	0.2918(4)	0.2919(5)	0.2925(5)
	y	0.33168(4)	0.3324(3)	0.3322(3)	0.3321(3)	0.3326(3)
	z	0.18937(5)	0.1911(7)	0.1906(6)	0.1910(7)	0.1915(7)
	B_{iso}	0.216(6)	0.35(3)	0.39(3)	0.38(3)	0.36(3)
O1	*x*	0.10933(12)	0.1092(11)	0.1096(10)	0.1085(13)	0.1089(12)
	y	0.14685(10)	0.1480(8)	0.1477(7)	0.1478(9)	0.1477(8)
	z	0.12866(14)	0.1296(13)	0.1308(12)	0.1299(15)	0.1322(15)
	B_{iso}	0.384(13)	0.37(8)	0.52(7)	0.53(8)	0.44(8)
O2	*x*	0.12287(12)	0.1215(11)	0.1223(0)	0.1213(13)	0.1209(12)
	y	0.68535(10)	0.6844(9)	0.6838(8)	0.6837(9)	0.6825(9)
	z	0.18113(14)	0.1786(14)	0.1786(12)	0.1780(15)	0.1780(14)
	B_{iso}	0.302(13)	0.46(8)	0.41(7)	0.50(9)	0.39(8)
O3	*x*	0.27507(12)	0.2748(12)	0.2762(10)	0.2763(13)	0.2764(14)
	y	0.45443(10)	0.4546(8)	0.4552(7)	0.4551(9)	0.4546(9)
	z	0.95474(14)	0.9550(14)	0.9556(12)	0.9547(16)	0.9538(16)
	B_{iso}	0.349(14)	0.42(7)	0.39(7)	0.43(8)	0.40(8)
O4	*x*	0.28353(12)	0.2837(11)	0.2838(10)	0.2838(12)	0.2844(11)
	y	0.93570(10)	0.9361(8)	0.9368(7)	0.9366(9)	0.9355(8)
	z	0.93567(14)	0.9367(13)	0.9372(13)	0.9376(14)	0.9380(14)
	B_{iso}	0.334(13)	0.44(8)	0.52(7)	0.35(8)	0.43(8)
O5	*x*	0.10836(12)	0.1080(11)	0.1082(10)	0.1083(13)	0.1090(11)
	y	0.15210(10)	0.1516(9)	0.1518(7)	0.1522(9)	0.1524(8)
	z	0.66671(14)	0.6670(13)	0.6679(14)	0.6671(16)	0.6697(14)
	B_{iso}	0.342(13)	0.46(9)	0.43(8)	0.50(9)	0.40(9)
O6	*x*	0.12192(12)	0.1213(12)	0.1216(10)	0.1203(14)	0.1209(15)
	y	0.63063(10)	0.6310(8)	0.6312(7)	0.6310(10)	0.6309(9)
	z	0.63939(14)	0.6403(16)	0.6400(14)	0.6400(17)	0.6401(18)
	B_{iso}	0.297(13)	0.45(7)	0.54(7)	0.34(8)	0.27(8)
O7	*x*	0.28226(12)	0.2821(11)	0.2817(10)	0.2822(12)	0.2839(12)
	y	0.44512(10)	0.4455(8)	0.4452(8)	0.4456(9)	0.4463(8)
	z	0.42868(14)	0.4297(13)	0.4921(12)	0.4292(14)	0.4299(14)
	B_{iso}	0.346(13)	0.45(8)	0.59(7)	0.48(9)	0.53(8)
O8	*x*	0.29156(12)	0.2915(11)	0.2923(10)	0.2925(13)	0.2924(12)
	y	0.94684(10)	0.9476(8)	0.9480(8)	0.9479(10)	0.9476(8)
	z	0.46574(14)	0.4657(13)	0.4659(12)	0.4657(15)	0.4651(14)
	B_{iso}	0.346(13)	0.44(8)	0.45(7)	0.43(8)	0.47(8)
O9	*x*	0.50074(12)	0.5005(10)	0.5005(10)	0.5011(12)	0.5018(12)
	y	0.27519(10)	0.2743(8)	0.2731(8)	0.2730(10)	0.2729(9)
	z	0.24405(13)	0.2445(13)	0.2440(12)	0.2439(15)	0.2438(15)
	B_{iso}	0.364(13)	0.57(8)	0.62(7)	0.48(9)	0.43(8)
O10	*x*	0.50154(11)	0.5015(12)	0.5013(10)	0.5012(13)	0.5013(13)
	y	0.23099(10)	0.2320(9)	0.2315(8)	0.2327(10)	0.2339(9)
	z	0.75595(13)	0.7555(14)	0.7553(13)	0.7555(16)	0.7559(15)
	B_{iso}	0.350(13)	0.57(8)	0.58(7)	0.47(8)	0.62(9)

Note: Units for B_{iso} are Å².

TABLE 3. Selected bond distances (Å) in kyanite at various pressures

Bond	0.00	1.35	2.54	3.73	4.56
			P (GPa)		
Al1-O2	1.873(1)	1.881(9)	1.869(8)	1.865(9)	1.866(9)
Al1-O6	1.885(1)	1.885(9)	1.880(8)	1.885(10)	1.879(11)
Al1-O7	1.972(1)	1.965(7)	1.961(7)	1.952(7)	1.946(7)
Al1-O8	1.986(1)	1.987(7)	1.986(7)	1.983(8)	1.978(7)
Al1-O9	1.848(1)	1.843(8)	1.845(8)	1.846(9)	1.839(9)
Al1-O10	1.850(1)	1.846(9)	1.841(8)	1.835(10)	1.834(9)
Avg.	1.902	1.901	1.897	1.894	1.890
Al2-O2	1.937(1)	1.929(9)	1.917(8)	1.914(9)	1.918(9)
Al2-O3	1.881(1)	1.876(7)	1.871(6)	1.869(7)	1.868(7)
Al2-O4	1.890(1)	1.887(7)	1.888(6)	1.883(7)	1.873(7)
Al2-O6	1.910(1)	1.900(9)	1.901(8)	1.912(10)	1.895(11)
Al2-O9	1.929(1)	1.926(8)	1.922(8)	1.914(9)	1.903(9)
Al2-O10	1.922(1)	1.921(9)	1.916(8)	1.899(10)	1.906(9)
Avg.	1.912	1.907	1.903	1.899	1.894
Al3-O2	1.984(1)	1.979(8)	1.979(8)	1.971(9)	1.968(9)
Al3-O3	1.924(1)	1.920(9)	1.922(8)	1.910(9)	1.909(10)
Al3-O5	1.860(1)	1.859(7)	1.855(6)	1.851(7)	1.846(7)
Al3-O6	1.881(1)	1.881(7)	1.878(6)	1.873(8)	1.872(7)
Al3-O6'	1.969(1)	1.964(9)	1.962(8)	1.955(10)	1.952(11)
Al3-O7	1.885(1)	1.877(8)	1.875(8)	1.873(9)	1.874(9)
Avg.	1.917	1.913	1.912	1.906	1.904
Al4-O1	1.816(1)	1.822(7)	1.817(6)	1.814(7)	1.807(7)
Al4-O1'	1.995(1)	1.988(8)	1.992(8)	1.987(9)	1.993(9)
Al4-O2	1.846(1)	1.844(7)	1.847(6)	1.844(7)	1.852(7)
Al4-O4	1.909(1)	1.901(8)	1.895(8)	1.889(9)	1.888(8)
Al4-O5	1.934(1)	1.925(8)	1.919(8)	1.920(9)	1.913(8)
Al4-O8	1.874(1)	1.875(8)	1.872(8)	1.862(9)	1.858(9)
Avg.	1.896	1.892	1.890	1.886	1.885
Si1-O4	1.631(1)	1.629(8)	1.629(7)	1.632(8)	1.636(8)
Si1-O5	1.642(1)	1.640(8)	1.638(7)	1.631(9)	1.627(8)
Si1-O8	1.622(1)	1.613(8)	1.604(7)	1.603(9)	1.605(8)
Si1-O10	1.645(1)	1.645(8)	1.640(7)	1.642(9)	1.643(8)
Avg.	1.635	1.632	1.628	1.627	1.628
Si2-O1	1.640(1)	1.639(7)	1.633(6)	1.633(8)	1.635(7)
Si2-O3	1.629(1)	1.630(8)	1.625(7)	1.628(9)	1.628(9)
Si2-O7	1.624(1)	1.619(8)	1.615(7)	1.611(8)	1.607(8)
Si2-O9	1.646(1)	1.639(7)	1.643(7)	1.643(9)	1.644(9)
Avg.	1.635	1.632	1.629	1.629	1.628

from the position of the R_1 laser-induced fluorescence peak, with an error of approximately 0.05 GPa. The fixed-ϕ mode of data measurement (Finger and King 1978) was used throughout the high-pressure experiments to maximize reflection accessibility and minimize attenuation by the diamond cell. Lattice constants were determined using the same method as described for the room-pressure experiment.

X-ray diffraction intensities were collected at 1.35, 2.54, 3.73, and 4.56 GPa for all accessible reflections with $0° \leq 2\theta \leq 60°$. The experimental procedures for X-ray data collection, reduction, and structure refinements were similar to those described above for the data collected in air. In addition, corrections were made for absorption by the diamond and beryllium components of the pressure cell. Owing to the limited reflection data, all atoms were refined with only isotropic displacement factors. Unit-cell dimensions and final refinement statistics are given in Table 1; atomic positional and isotropic displacement parameters are listed in Table 2; selected interatomic distances are presented in Table 3 and polyhedral volumes and distortion indices in Table 4.

TABLE 4. Polyhedral volumes (Å³) and distortion indices of kyanite at various pressures

Polyhedron		P (GPa)				
		0.00	1.35	2.54	3.73	4.56
Al1O$_6$	V*	8.983(4)	8.97(4)	8.92(4)	8.89(5)	8.83(5)
	QE	1.0154(1)	1.0149(5)	1.0145(5)	1.0141(6)	1.0140(6)
	AV	47.6(1)	46.0(9)	44.6(8)	43.6(9)	43.3(9)
Al2O$_6$	V	9.122(4)	9.07(4)	9.01(4)	8.96(5)	8.89(5)
	QE	1.0140(1)	1.0130(5)	1.0129(5)	1.0123(5)	1.0122(5)
	AV	50.1(1)	46.6(9)	46.2(9)	44.0(9)	43.8(9)
Al3O$_6$	V	9.158(4)	9.11(4)	9.09(4)	9.01(5)	8.97(5)
	QE	1.0178(1)	1.0173(6)	1.0174(5)	1.0168(6)	1.0171(6)
	AV	56.3(1)	55.0(9)	55.0(8)	53.3(9)	54.3(9)
Al4O$_6$	V	8.917(4)	8.88(4)	8.85(4)	8.79(5)	8.78(4)
	QE	1.0137(1)	1.0125(4)	1.0124(4)	1.0128(4)	1.0128(4)
	AV	41.9(1)	38.6(6)	38.0(6)	39.6(7)	39.3(7)
Si1O$_4$	V	2.239(1)	2.23(1)	2.21(1)	2.21(2)	2.21(2)
	QE	1.0011(1)	1.0011(2)	1.0012(2)	1.0023(2)	1.0015(2)
	AV	4.2(4)	4.2(4)	4.3(4)	4.6(4)	5.6(4)
Si2O$_4$	V	2.236(1)	2.22(1)	2.21(1)	2.21(2)	2.21(2)
	QE	1.0017(1)	1.0017(3)	1.0017(3)	1.0016(3)	1.0016(3)
	AV	6.6(5)	6.7(6)	6.4(5)	6.1(6)	6.0(5)

* V = polyhedral volume; QE = quadratic elongation; AV = angle variance (Robinson et al. 1971).

RESULTS

Unit-cell compressibilities and bulk modulus

All unit-cell parameters vary linearly with pressure, among which a, b, c, β, and γ decrease with increasing pressure, whereas α increases; however, cell compression is only slightly anisotropic. Because kyanite is triclinic, the compressional anisotropy of the crystal can be better described by strain tensors. Unit-strain tensors of kyanite at various pressures were calculated from each data point relative to the room-pressure unit-cell parameters using the STRAIN program written by Y. Ohashi (Hazen and Finger 1982). The magnitudes of the principal strain coefficients are plotted in Figure 2 as a function of pressure. Lines superimposed in Figure 2 represent weighted least-squares fits to the data, yielding $|\epsilon_1| = 0.00145(2) -$

$0.000010(4)P$ (GPa^{-1}), $|\epsilon_2| = 0.00168(2) - 0.000001(5)P$ (GPa^{-1}), and $|\epsilon_3| = 0.00193(6) - 0.000014(18)P$ (GPa^{-1}). Note that data at 0.65 and 1.35 GPa were ignored in the fitting because of their large uncertainties. The magnitudes of the longest and the shortest axes of the strain ellipsoid show a slight decrease with increasing pressure, whereas that of the intermediate axis is virtually unchanged. The negative slopes for $|\epsilon_1|$ and $|\epsilon_3|$ reflect the stiffening of the structure in these directions at higher pressures. The orientation of the strain ellipsoid does not change significantly with pressure. At 4.56 GPa, the major axes of the strain ellipsoid are oriented at 95(3), 34(2), and 24(2)°, with respect to a, b, and c; 20(5), 91(4), and 88(5)°; and 109(5), 56(2), and 34(2)° for ϵ_1, ϵ_2, and ϵ_3, respectively. The most compressible direction corresponds approximately to the [012] direction.

The unit-cell volume of kyanite changes linearly with pressure up to 4.56 GPa. Weighted volume and pressure data fitted to a second-order Birch-Murnaghan equation of state ($K' = 4.0$) yields $V_0 = 293.32(2)$ Å³ and $K_0 = 193(1)$ GPa.

Structural variations with pressure

From a crystal chemistry standpoint, four distinct AlO$_6$ octahedra in kyanite at room pressure may be divided into two different groups: Al1 with Al4, and Al2 with Al3. The two octahedra in each group are similar in terms of mean Al-O bond distances (Table 3), octahedral volumes and distortion indices (Table 4), as well as the site energies (Smyth and Bish 1988). In comparison with the Al1 and Al4 octahedra, the Al2 and Al3 octahedra exhibit relatively large average Al-O bond lengths and volumes. In addition, they appear to be more distorted than the Al1 and Al4 octahedra (Table 4).

At high pressures, no dominant compression directions are apparent for the four AlO$_6$ octahedra. As pressure increases, the average Al-O bond lengths of all octahedra
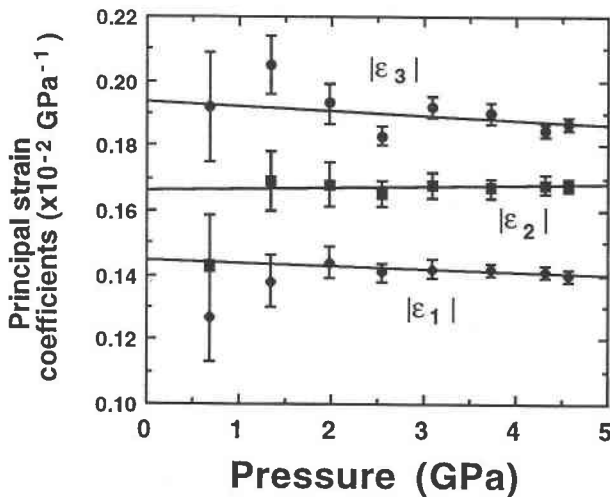

FIGURE 2. The magnitudes of the principal unit-strain coefficients as a function of pressure. The solid lines represent the best linear fits to the data.
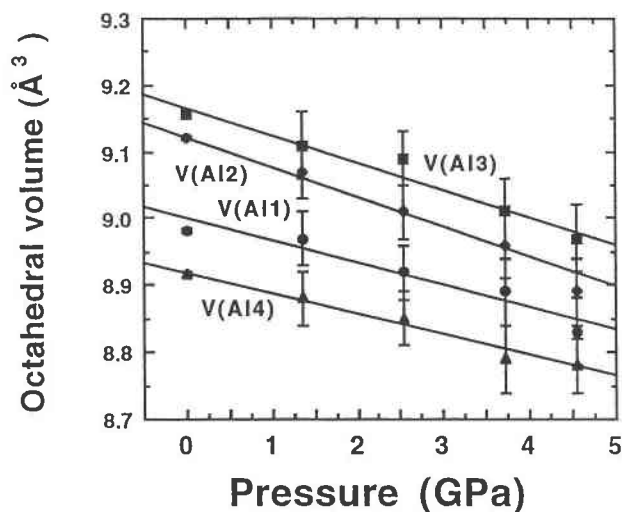
FIGURE 3. Variations of AlO_6 octahedral volumes in kyanite with pressure.

decrease linearly, with the longer mean Al2-O and Al3-O distances decreasing more than the shorter mean Al1-O and Al4-O distances. The linear compressibilities of the four mean Al-O bond lengths are in the order: β_{Al2-O} [1.98(12) $\times$ 10^{-3} GPa^{-1}] > β_{Al3-O} [1.49(18) $\times$ 10^{-3} GPa^{-1}] > β_{Al1-O} [1.39(19) $\times$ 10^{-3} GPa^{-1}] > β_{Al4-O} [1.29(8) $\times$ 10^{-3} GPa^{-1}]. However, linear compressibilities of individual Al-O bond lengths are not always a direct function of magnitude. For instance, within the Al1 octahedron, the Al1-O8 distance is always longer than the Al1-O7 distance throughout the pressure range of the experiment, but the linear compressibility of the Al1-O7 bond length is about three times that of the Al1-O8 distance (2.84 $\times$ 10^{-3} vs. 0.83 $\times$ 10^{-3} GPa^{-1}). Furthermore, within the Al4 octahedron, the Al4-O1 bond distance is the longest of all Al-O distances, but it remains essentially unchanged up to 4.56 GPa. Similar results were also observed in andalusite (Ralph et al. 1984). All four octahedra become less distorted at higher pressures (Table 4). Volumes of the four AlO_6 octahedra decrease nearly linearly with increasing pressure and the rates of decrease are greater for the relatively larger Al2 and Al3 octahedra than for the Al1 and Al4 octahedra (Fig. 3). The bulk moduli for the Al1, Al2, Al3, and Al4 octahedra are 273(43), 207(14), 224(26), and 281(24) GPa, respectively.

Two crystallographically distinct SiO_4 tetrahedra in kyanite at room pressure display very similar configurations, as indicated by mean Si-O bond lengths (Table 3), tetrahedral volumes, and distortion indices (Table 4). These similarities are maintained at higher pressures, and the two tetrahedra remain fairly regular within the experimental pressure range. The mean Si-O bond lengths of both tetrahedra decrease slightly from 1.635 Å at room pressure to 1.628 Å at 4.56 GPa with a linear compressibility of ~1.00(20) $\times$ 10^{-3} GPa^{-1}. Compression of the Si-O bond lengths was also observed in andalusite (Ralph

et al. 1984) and other silicate minerals (Levien and Prewitt 1981; Hazen and Finger 1978). The bulk moduli for the Si1 and Si2 tetrahedra are 322(80) and 400(95) GPa, respectively.

DISCUSSION

Vaughan and Weidner (1978) measured elastic constants of andalusite and sillimanite using the Brillouin scattering method. Their results show that c_{33}, the incompressibility along the c axis, in both crystals is much greater than either c_{11} or c_{22} (c_{11} = 233.4, c_{22} = 289.0, and c_{33} = 380.1 GPa for andalusite and c_{11} = 287.3, c_{22} = 231.9, and c_{33} = 388.4 GPa for sillimanite), suggesting a strong anisotropy of compressibility for the two crystals. The bulk moduli (the Reuss bound values) given by Vaughan and Weidner (1978) for andalusite and sillimanite are 158 and 166 GPa, respectively. The axial-compression ratios of $\beta_a:\beta_b:\beta_c$ for andalusite determined by Ralph et al. (1984) are 2.1:1.5:1.0 and the bulk modulus is 139(10) GPa. In comparison with andalusite and sillimanite, kyanite shows a much less anisotropic compressibility and a larger bulk modulus, which may contribute to its stability at high pressures. Winter and Ghose (1979) found that kyanite also shows considerably less anisotropy of thermal expansion at high temperature than either andalusite or sillimanite. The relatively large bulk modulus for kyanite is expected because its structure is more densely packed than that of andalusite or sillimanite. From measurements on properties of the hot-pressed samples of the aggregate, a mixture of the unknown mineral (kyanite, sillimanite, or andalusite) and a ductile solid of known characteristics, Brace et al. (1969) derived a bulk modulus of 130(10) GPa for all three Al_2SiO_5 polymorphs. The uncertainties in compressibility determined by this technique could be large because of difficulties in finding a close match of the known matrix and the unknown mineral. Thus the data reported by Brace et al. (1969) for kyanite, sillimanite, and andalusite are excluded from the following discussion. On the basis of molecular dynamics calculation, Matsui (1996) derived a bulk modulus of 197 GPa for kyanite, which is in good agreement with our result. Figure 4 illustrates the relationship between bulk moduli and molar volumes for andalusite, sillimanite, and kyanite. Within the experimental errors, the bulk moduli of the Al_2SiO_5 polymorphs appear to decrease linearly as the molar volumes, V_m, increase with K_0 = 453 − 5.8V_m. The significantly less anisotropic compressibility of kyanite stems from the fact that its structure is nearly a cubic close-packed arrangement of O atoms and that the four AlO_6 octahedra share several edges in a quite complex manner (five each for the Al1 and Al3 octahedra and four each for the Al2 and Al4 octahedra) (Fig. 1). These structural features not only result in more uniformly distributed compression (or thermal expansion) of the structure, but also they yield no clearly dominant octahedral compression directions. In contrast, running parallel to c are two types of polyhedral chains in andalusite and sillimanite. In addition to chains of edge-shared
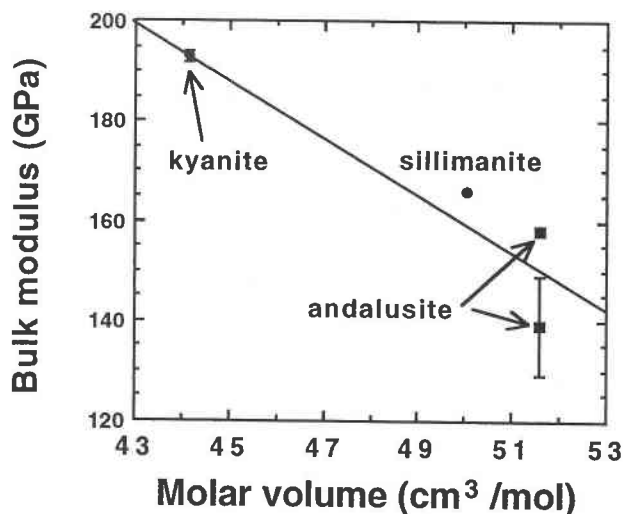
FIGURE 4. The relationship between the bulk moduli of the three Al₂SiO₅ polymorphs and their molar volumes. Molar volumes are 44.158, 50.052, and 51.572 cm³/mol for kyanite, sillimanite, and andalusite, respectively. The bulk moduli for three polymorphs are taken from Vaughan and Weidner (1978), Ralph et al. (1984), and the present study.

FIGURE 5. The bulk modulus-volume relationship for AlO₆ octahedra in kyanite and andalusite.

AlO₆ octahedra in both structures, there are also fully extended double chains consisting of corner-shared SiO₄ tetrahedra and AlO₅ hexahedra in andalusite or SiO₄ and AlO₄ tetrahedra in sillimanite (see Figs. 4 and 5 of Vaughan and Weidner 1978). These two types of chains in both crystal structures are linked together through sharing of polyhedral corners. The structures of andalusite and sillimanite are less compressible along c than along a or b because the polyhedral chains become the load-bearing framework along c.

As shown above, kyanite compression appears to be complicated by the triclinic symmetry and the variety of polyhedral units. We reduce this complication by examining the compression simply as a function of O-O contacts in terms of closest packing, because the kyanite structure can be considered as a distorted cubic closest packing of O atoms with monolayers stacked along the [012] direction. The distortion in the packing is due to mismatched sizes of SiO₄ and AlO₆ groups as well as narrow O-O contacts required by edge-sharing polyhedra. The AlO₆ octahedra appear to become more regular with increasing pressure, indicating that distortion in the closest packing may decrease with pressure. Accordingly, we analyzed the distortion of the closest packing in kyanite. To do this, we developed a closest-packing distortion parameter, U_{cp}, which is defined as the average squared displacement of the observed O atoms in kyanite from their ideal closest packed analogs. An ideal closest-packed array was associated with the O atoms in kyanite by minimizing the sum of the squared displacements between observed and ideal positions, while varying the ideal closest-packed O atom radius, the orientation of the closest-packed layers, and a translation vector that relates the
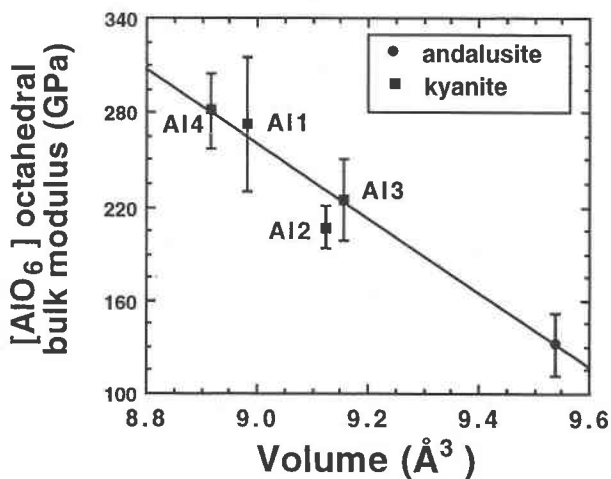
origin of the two systems. The U_{cp} parameter has a value of zero if the observed atoms exactly occupy the closest-packed positions. If the positions of the O atoms in kyanite had been refined in an ideal closest-packed array, with only one nonequivalent O atom, then the equivalent isotropic displacement factor because of static disorder would be similar in value to this distortion parameter. The refined values of U_{cp} and the ideal O atom radius for the kyanite structure at various temperatures and pressures are presented in Table 5. The high-temperature data were taken from Winter and Ghose (1979).

An examination of Table 5 shows that U_{cp} decreases with increasing pressure, indicating that the distortion from closest-packing in kyanite decreases with increasing pressure. Furthermore, the radii of the ideal closest-packed spheres also decrease with pressure: $r = 1.37237(8) - 0.00225(3)P$. Note that the most compressible direction in the kyanite structure corresponds to the direction along which the closest-packed monolayers are stacked. This direction is approximately equivalent to [1̄22] from which the d value, equal to the separation between three monolayers, is related to the radius of the ideal closest packing spheres by $r = \sqrt{6}\,d/4$. Using the d value of 2.2726 Å at $P = 0$ GPa, we obtain a value for

TABLE 5. The closest-packing distortion parameter (U_{cp}) and the ideal closest-packed O atom radius in kyanite at various pressures and temperatures

P-T	U_{cp}	Radius (Å)
0.00 GPa	0.0658	1.372
1.35 GPa	0.0635	1.369
2.54 GPa	0.0631	1.367
3.73 GPa	0.0614	1.364
4.56 GPa	0.0607	1.362
25 °C	0.0652	1.373
400 °C	0.0692	1.374
600 °C	0.0689	1.379

Note: High-temperature data taken from Winter and Ghose (1979).

$r = 1.392$ Å. This value is 0.02 Å larger than the average O atom radius for the entire structure, suggesting that the O atoms between separate monolayers are separated from each other by a larger amount than within the monolayers. This difference explains why the largest compressibility of the structure is in the [012] direction. From the closest-packing point of view, the compressibility of the kyanite structure is determined largely by the O-O nearest neighbor contacts, with both the degree of distortion from closest packing and the radii of the O atoms decreasing with increasing pressure. The details of how the O atoms become more closest packed is determined by the Al-O and Si-O linkages, with Al-O weaker than Si-O.

Linear compressibilities of the four average Al-O bond lengths in kyanite are similar to those of pyrope and grossular [$1.9 (3) \times 10^{-3}$ GPa^{-1}] (Hazen and Finger 1978) and of ruby [$1.2(1) \times 10^{-3}$ GPa^{-1}] (Finger and Hazen 1978), but differ from the greater average Al-O linear compressibility of andalusite [$2.5(2) \times 10^{-3}$ GPa^{-1}] (Ralph et al. 1984). Similarly, the average value of the four AlO_6 octahedral bulk moduli in kyanite [247(27) GPa] is comparable with the AlO_6 octahedral bulk moduli of 240(20) GPa for ruby (Finger and Hazen 1978) and 220(50) GPa for both pyrope and grossular (Hazen and Finger 1978), but are larger than the octahedral bulk modulus of 132(20) GPa determined for andalusite (Ralph et al. 1984). The appreciably larger AlO_6 octahedron in andalusite, as indicated by its mean Al-O bond length of 1.935 Å and octahedral volume of 9.538 Å^3, may be responsible for its small octahedral bulk modulus. Figure 5, which plots the AlO_6 octahedral bulk moduli of kyanite and andalusite against their octahedral volumes at room pressure, shows that the AlO_6 octahedral bulk modulus is inversely proportional to its volume. If we assume that the linear bulk modulus–volume relationship illustrated in Figure 5 also holds for sillimanite, then the bulk modulus of the AlO_6 octahedron in sillimanite is estimated to be ~213(45) GPa, given its octahedral volume of 9.173 Å^3 (Winter and Ghose 1979). More research on the compressibility and the crystal structure of sillimanite at high pressure will help us to understand better the high-pressure crystal chemistry of the Al_2SiO_5 system.

One of the noteworthy features of the kyanite structure is the complexity of the edge sharing among four AlO_6 octahedra. It is, therefore, interesting to compare compressibilities of edge-shared O-O distances and with unshared O-O distances. As expected, the average shared O-O distance for each octahedron is about two to three times less compressible than the unshared O-O distance. The linear compressibilities of the average unshared O-O distances for the Al1, Al2, Al3, and Al4 octahedra are $1.75(16) \times 10^{-3}$, $2.26(13) \times 10^{-3}$, $1.91(23) \times 10^{-3}$, and $1.70(11) \times 10^{-3}$ GPa^{-1}, respectively, whereas those of the average shared O-O distances are $0.62(28) \times 10^{-3}$, $1.18(15) \times 10^{-3}$, $1.13(19) \times 10^{-3}$, and $0.60(33) \times 10^{-3}$ GPa^{-1}, respectively. Because of the differential O-O distance compression, the differences between the shared and unshared O-O distances for each octahedron decrease

as pressure increases, accounting in part for the fact that all octahedra become more regular at higher pressures. Note that the respective linear compressibilities of the shared and unshared O-O distances are nearly identical for the Al1 and Al4 octahedra, and those for the Al2 and Al3 octahedra are very similar. Moreover, like the mean Al-O bond lengths, both average unshared and shared O-O distances for the Al2 and Al3 octahedra are more compressible than those for the Al1 and Al4 octahedra.

In many compounds, structural variations with increasing temperature are opposite to those observed with increasing pressure (Hazen and Finger 1982). Ralph et al. (1984) have demonstrated that this inverse relationship does not strictly hold for andalusite. For kyanite, the inverse relationship is also only qualitatively true for the structural changes in bond lengths, bond angles, and polyhedral volumes. A comparison of our results with high-temperature data determined by Winter and Ghose (1979) for kyanite indicates that the most and the least thermally expandable directions in the kyanite structure correspond approximately to the most and the least compressible directions, respectively. However, it is uncertain whether the changes in all six triclinic unit-cell dimensions follow the inverse relationship because of the disagreement in high-temperature data. Skinner et al. (1961) observed an increase of the γ angle at elevated temperatures by powder X-ray diffraction, whereas Winter and Ghose (1979) found a slight decrease of γ using single-crystal X-ray diffraction. Although our data could be consistent with the observation of Skinner et al. (1961), provided that the inverse relationship is held, more investigations are needed on kyanite as a function of temperature.

CONCLUSIONS

After reviewing high-pressure structural data, Hazen and Finger (1985) concluded that most crystal compression can be accounted for principally by three types of changes in structural geometry: polyhedral compression, bond-angle bending, and intermolecular compression. To a first approximation, our results show that the high-pressure behavior of the AlO_6 octahedra, in particular the Al-O bond compression, controls the compression of the kyanite structure. This behavior is consistent with the conclusion of Hazen and Finger (1985) that bond-angle bending and intermolecular changes cannot be major factors dominating compression of crystals with close-packed structures. However, the significantly differential compression of the shared and unshared O-O distances for each AlO_6 octahedron suggests that polyhedral distortion can also be an important compression mechanism in close-packed, relatively incompressible structures. Accordingly, it is necessary to examine other dense silicate minerals (such as olivine and wadsleyite) carefully to discern the subtle role of polyhedral distortion in crystal compression.

REFERENCES CITED

Becker, P.J. and Coppens, P. (1975) Extinction within the limit of validity of the Darwin transfer equations: III. Non-spherical crystals and anisotropy of extinction. Acta Crystallographica, A31, 417–425.

Brace, W.F., Scholz, C.H., and La Mori, P.N. (1969) Isothermal compressibility of kyanite, andalusite, and sillimanite from synthetic aggregates. Journal of Geophysical Research, 74, 2089–2098.

Burnham, C.W. (1963) Refinement of the crystal structure of kyanite. Zeitschrift für Kristallographie, 118, 337–360.

Finger, L.W. and Hazen, R.M. (1978) Crystal structure and compressibility of ruby to 46 kbar. Journal of Applied Physics, 49, 5823–5826.

Finger, L.W. and King, H. (1978) A revised method of operation of the single-crystal diamond cell and refinement of the structure of NaCl at 32 kbar. American Mineralogist, 63, 337–342.

Finger, L.W. and Prince, E. (1975) A system of FORTRAN IV computer programs for crystal structure computations. National Bureau of Standards Technology Note 854.

Hazen, R.M. and Finger, L.W. (1978) Crystal structures and compressibilities of pyrope and grossular to 60 kbar. American Mineralogist, 63, 297–303.

———(1982) Comparative Crystal Chemistry. Wiley, New York.

———(1985) Crystals at high pressure. Scientific American, 252, 110–117.

Hemingway, B.S., Robie, R.A., Evans, H.T., and Kerrick, D.M. (1991) Heat capacities and entropies of sillimanite, fibrolite, andalusite, kyanite, and quartz and the Al_2SiO_5 phase diagram. American Mineralogist, 76, 1597–1613.

Ibers, J.A. and Hamilton, W.C. (1974) International tables for X-ray crystallography. Vol. IV, 366 p. Kynoch, Birmingham, U.K.

Kerrick, D.M. (1990) The Al_2SiO_5 polymorphs. In Mineralogical Society of America Reviews in Mineralogy, 22, 1–406.

King, H.E. and Finger, L.W. (1979) Diffracted beam crystal centering and its application to high-pressure crystallography. Journal of Applied Crystallography, 12, 374–378.

Lehmann, M.S. and Larsen, F.K. (1974) A method for location of the peaks in step-scan-measured Bragg reflexions. Acta Crystallographica, A30, 580–584.

Levien, L. and Prewitt, C.T. (1981) High-pressure structural study of diopside. American Mineralogist, 66, 315–323.

Mao, H.K., Xu, J., and Bell, P.M. (1986) Calibration of the ruby pressure gauge to 800 kbar under quasi-hydrostatic conditions. Journal of Geophysical Research, 91, 4673–4676.

Matsui, M. (1996) Molecular dynamics study of the structures and bulk moduli of crystals in the system $CaO-MgO-Al_2O_3-SiO_2$. Physics and Chemistry of Minerals, 23, 345–353.

Náray-Szabo, St., Taylor, W.H., and Jackson, W.W. (1929) The structure of kyanite. Zeitschrift für Kristallographie, 71, 117–130.

Papike, J.J. and Cameron, M. (1976) Crystal chemsitry of silicate minerals of geophysical interest. Reviews in Geophysics and Space Physics, 14, 37–80.

Ralph, R.L., Finger, L.W., Hazen, R.M., and Ghose S. (1984) Compressibility and crystal structure of andalusite at high pressure. American Mineralogist, 69, 513–519.

Ribbe, P.H. (1980) Aluminum silicate polymorphs and mullite. In Mineralogical Society of America Reviews in Mineralogy, 5, 189–214.

Robie, R.A. and Hemingway, B.S. (1984) Entropies of kyanite, andalusite, and sillimanite: additional constraints on the pressure and temperature of the Al_2SiO_5 triple point. American Mineralogist, 69, 298–306.

Robinson, K., Gibbs, G.V., and Ribbe, P.H. (1971) Quadratic elongation: A quantitative measure of distortion in coordination polyhedra. Science, 172, 567–570.

Skinner, B.J., Clark, S.P., and Appleman, D.E. (1961) Molar volumes and thermal expansions of andalusite, kyanite, and sillimanite. American Journal of Sciences, 259, 651–668.

Smyth, J.R. and Bish, D.L. (1988) Crystal structures and cation sites of the rock-forming minerals. Allen and Unwin, Boston, Massachusetts.

Vaughan, M.T. and Weidner, D.J. (1978) The relationships of elasticity and crystal structure in andalusite and sillimanite. Physics and Chemistry of Minerals, 3, 133–144.

Winter, J.K. and Ghose, S. (1979) Thermal expansion and high-temperature crystal chemistry of the Al_2SiO_5 polymorphs. American Mineralogist, 64, 573–586.